

A Search for Vector Diquarks at the CERN LHC

E. Arik^a, O. Çakır^b, S. A. Çetin^a and S. Sultansoy^{c,d}

^a Bogazici University, Faculty of Sciences, Department of Physics,
80815, Bebek, Istanbul, Turkey

^b Ankara University, Faculty of Sciences, Department of Physics,
06100 Tandogan, Ankara, Turkey

^c Gazi University, Faculty of Arts and Sciences, Department of Physics,
06500, Teknikokullar, Ankara, Turkey

^d Azerbaijan Academy of Sciences, Institute of Physics,
H. Cavid av., 33, Baku, Azerbaijan

Abstract

Resonant production of the first generation vector diquarks at the CERN Large Hadron Collider (LHC) is investigated. It is shown that the LHC will be able to discover vector diquarks with masses up to 9 TeV for quark-diquark-quark coupling $\alpha_D = 0.1$ and 4 TeV for $\alpha_D = 5 \times 10^{-4}$.

The existence of at least three fermion families and especially inter-family mixings naturally lead to the hypothesis that they are made up of more fundamental constituents frequently called preons [1]. Today, the compositeness should be considered as a candidate for beyond the standard model (BSM) physics on the same footing as SUSY. Moreover, some assumptions made in order to get rid of huge number of free parameters in three family minimal supersymmetric standard model (MSSM) have natural explanation (see [2] and references therein) in the framework of preonic models. These models predict a rich spectrum of new particles with unusual quantum numbers at high energies such as excited quarks and leptons, diquarks, dileptons, leptoquarks, leptogluons, sextet quarks, octet bosons etc. In preonic models, diquarks are as natural as leptoquarks [3]. They are colored objects having integer-spin and baryon number $|B| = 2/3$ or 0. Diquarks are also predicted in the framework of superstring-inspired E_6 models [4].

Recent collider limits on the diquark masses come from Tevatron data which exclude the region $290 < M_D < 420$ GeV (for E_6 diquarks) [5]. Diquark production at e^+e^- colliders, ep colliders and $p\bar{p}$ colliders have been analyzed in [6], [7]

and [8] respectively. The resonance production of scalar diquarks at CERN LHC has been studied in [9].

In this work, we study composite vector diquark production at the LHC. Interaction Lagrangian and quantum numbers of diquarks are discussed. Decay width and production cross section of vector diquarks at the LHC are considered. Vector diquark signal and corresponding backgrounds are analyzed.

A model independent, baryon number conserving, most general $SU(3)_C \times SU(2)_W \times U(1)_Y$ invariant effective Lagrangian for diquarks has the form

$$\begin{aligned}
L_{|B|=0} = & f_{1L}\bar{q}_L\gamma^\mu q_L D_{1\mu}^c + (f_{1R}\bar{d}_R\gamma^\mu d_R + f'_{1R}\bar{u}_R\gamma^\mu u_R)D_{1\mu}^{c'} \\
& + \tilde{f}_{1R}\bar{u}_R\gamma^\mu d_R\tilde{D}_{1\mu}^c + f_{3L}\bar{q}_L\tau^\mu q_L \cdot \mathbf{D}_{3\mu}^c \\
& + f_2\bar{q}_L i\tau_2 u_R D_2^c + \tilde{f}_2\bar{q}_L i\tau_2 d_R \tilde{D}_2^c + H.c.
\end{aligned} \tag{1}$$

$$\begin{aligned}
L_{|B|=2/3} = & (g_{1L}\bar{q}_L^c i\tau_2 q_L + g_{1R}\bar{u}_R^c d_R)D_1^c + \tilde{g}_{1R}\bar{d}_R^c d_R \tilde{D}_1^c \\
& + \tilde{g}'_{1R}\bar{u}_R^c u_R \tilde{D}_1^{c'} + g_{3L}\bar{q}_L^c i\tau_2 \tau q_L \cdot \mathbf{D}_3^c \\
& + g_2\bar{q}_L^c \gamma^\mu d_R D_{2\mu}^c + \tilde{g}_2\bar{q}_L^c \gamma^\mu u_R \tilde{D}_{2\mu}^c + H.c.
\end{aligned} \tag{2}$$

Diquarks with baryon number $B = 0$ are familiar fields, as they resemble the electroweak gauge vectors, and the neutral and charged Higgs scalars. Here, we consider only $|B| = 2/3$ vector diquarks. In Eq. (2), $q_L = (u_L, d_L)$ and $q^c = C\bar{q}^T$ ($\bar{q}^c = -q^T C^{-1}$). For the sake of simplicity, color and generation indices are omitted. Scalar diquarks $D_1, \tilde{D}_1, \tilde{D}_1^{c'}$ are $SU(2)_W$ singlets and \mathbf{D}_3 is $SU(2)_W$ triplet. Vector diquarks D_2 and \tilde{D}_2 are $SU(2)_W$ doublets. Diquarks may transform as anti-triplet or sextet under $SU(3)_C$. At this stage, we assume that each SM generation has its own diquarks and couplings in order to avoid flavour changing neutral currents.

Lagrangian (2) can be rewritten in the following more transparent form:

$$L = L_S + L_V \tag{3}$$

$$\begin{aligned}
L_S = & \left[g_{1L} (\bar{u}^c P_L d - \bar{d}^c P_L u) + g_{1R} \bar{u}^c P_R d \right] D_1 + \tilde{g}_{1R} \bar{d}^c P_R d \tilde{D}_1 \\
& + \tilde{g}'_{1R} \bar{u}^c P_R u \tilde{D}_1^{c'} + \sqrt{2}g_{3L} \bar{u}^c P_L u D_3^+ - \sqrt{2}g_{3L} \bar{d}^c P_L d D_3^- \\
& - g_{3L} (\bar{u}^c P_L d + \bar{d}^c P_L u) D_3^0 + H.c.
\end{aligned} \tag{4}$$

$$\begin{aligned}
L_V = & g_2 \bar{u}^c \gamma^\mu P_R d D_{2\mu}^{1c} + g_2 \bar{d}^c \gamma^\mu P_R u D_{2\mu}^{2c} + \tilde{g}_2 \bar{u}^c \gamma^\mu P_R u \tilde{D}_{2\mu}^{1c} \\
& + \tilde{g}_2 \bar{d}^c \gamma^\mu P_R d \tilde{D}_{2\mu}^{2c} + H.c.
\end{aligned} \tag{5}$$

where $P_L = (1 - \gamma_5)/2$ and $P_R = (1 + \gamma_5)/2$. A general classification of the first generation, color $\bar{3}$ diquarks is shown in Table 1.

For the present analysis, we consider the color $\bar{3}$ vector diquark D_2 with charge $1/3$ which couples to ud -pair as described by the effective Lagrangian (5). The decay width Γ_D , derived from the same Lagrangian, is

$$\Gamma_D = \frac{\alpha_D M_D}{9} \simeq 11 \text{ GeV} \left(\frac{M_D}{1 \text{ TeV}} \right) \quad \text{for } \alpha_D = 0.1 \quad , \quad (6)$$

where $\alpha_D = g_2^2/4\pi$, M_D is the mass of vector diquark. We use the narrow width approximation and consider this as long as $\Gamma_D/M_D < 0.1$. The cross section of the s-channel diquark resonance production can be obtained as

$$\sigma(pp \rightarrow D_2 X) = \sigma_0 \int_{M_D^2/s}^1 \frac{dx}{x} f_u(x, Q^2) f_d\left(\frac{M_D^2}{sx}, Q^2\right) \quad (7)$$

with

$$\sigma_0 = \frac{8\pi^2 \alpha_D}{9s} \quad (8)$$

where the factorization scale $Q^2 = M_D^2$, f_u and f_d are quark distribution functions of each proton. In Fig. 1, using the CTEQ5L quark distribution functions [10], the cross section versus diquark mass is plotted for LHC energy ($\sqrt{s} = 14$ TeV) with $\alpha_D = 0.1$.

D_2 -type diquark will decay via $D_2 \rightarrow ud$. Therefore, the signal will contain two hard jets in the final state. At LHC energy, major QCD processes contributing to two jet (jj) final states and their integrated cross sections are given in Table 2. The values in Table 2 have been generated by PYTHIA 6.1 [11] at parton level with various p_T cuts. It is clear that higher p_T cuts reduce the background cross sections significantly. These p_T cuts can be translated into the rapidity cuts via the relation between the p_T of a jet and the rapidity y given by $p_T = M_{jj}/2 \cosh y$.

The differential cross section as a function of the dijet invariant mass M_{jj} , with the rapidity cut $|y_{1,2}| \leq Y$, where y_1 and y_2 are rapidities of the massless final quarks, is given by

$$\begin{aligned} \frac{d\sigma}{dM_{jj}} &= \frac{M_{jj}^3}{2s} \int_{-Y}^Y dy_2 \int_{y_1^{\min}}^{y_1^{\max}} dy_1 \frac{1}{\cosh^2 y^*} \\ &\times [f_{u/A}(x_u, Q^2) f_{d/B}(x_d, Q^2) \frac{d\hat{\sigma}}{d\hat{t}}(\hat{s}, \hat{t}, \hat{u}) \\ &+ f_{d/A}(x_d, Q^2) f_{u/B}(x_u, Q^2) \frac{d\hat{\sigma}}{d\hat{t}}(\hat{s}, \hat{u}, \hat{t})] \end{aligned} \quad (9)$$

with

$$\begin{aligned} x_u &= \sqrt{\tau} e^{y^b}, & x_d &= \sqrt{\tau} e^{-y^b} \\ \hat{s} &= x_u x_d s, & \hat{t} &= -x_u p_T \sqrt{s} e^{-y_1}, & \hat{u} &= -x_d p_T \sqrt{s} e^{y_1} \\ y^* &= (y_1 - y_2)/2, & y^b &= (y_1 + y_2)/2 \\ y_1^{\min} &= \max(-Y, \log \tau - y_2), & y_1^{\max} &= \min(Y, -\log \tau - y_2), & \tau &= M_{jj}^2/s. \end{aligned}$$

In Eq. (9), the differential cross section for the subprocess $ud \rightarrow ud$ has the form

$$\begin{aligned} \frac{d\hat{\sigma}}{d\hat{t}}(ud \rightarrow ud) &= \frac{4\pi}{9} \left[\frac{\alpha_D^2 (\hat{s} + \hat{t})^2}{\hat{s}^2 [(\hat{s} - M_D^2)^2 + M_D^2 \Gamma_D^2]} \right. \\ &\quad \left. + \frac{2\alpha_s^2 (2\hat{s}^2 + \hat{t}^2 + 2\hat{s}\hat{t})}{\hat{s}^2 \hat{t}^2} - \frac{2\alpha_D \alpha_s}{\hat{t}} \frac{(\hat{s} + \hat{t})^2 (\hat{s} - M_D^2)}{\hat{s}^2 [(\hat{s} - M_D^2)^2 + M_D^2 \Gamma_D^2]} \right] \end{aligned} \quad (10)$$

where the dominant interference with the the t-channel gluon exchange is taken into account.

Fig. 2 shows jet-jet invariant mass distribution for the process $pp \rightarrow D_2 \rightarrow jjX$ together with the estimations of the QCD backgrounds at LHC. For comparison, signal peaks for vector diquark masses $M_D = 2, 4, 6, 8$ TeV and $\alpha_D = 0.1$ are superimposed on the background distribution.

We have estimated background events for an integrated LHC luminosity of 10^5 pb^{-1} taking into account, as an example, the energy resolution of ATLAS hadronic calorimeter [12]:

$$\frac{\delta E}{E} = \frac{50\%}{\sqrt{E}} + 3\% \quad (11)$$

for jets with $|y| < 3$. The mass resolution can be expressed as

$$\frac{\Delta M}{M} \approx \frac{\delta E}{\sqrt{2E}} \quad (12)$$

We have chosen ΔM as the mass window centered at M_D for signal and background estimations. Here, we take the energy of a jet $E \approx M_D/2$. For signal estimation the mass window ΔM is taken to be $2\Gamma_D$. This corresponds to the 95% CL for statistical acceptance. The cross sections are calculated by using the formula

$$\sigma = \int_{M_D - \Delta M/2}^{M_D + \Delta M/2} dM_{jj} \left(\frac{d\sigma}{dM_{jj}} \right) \quad (13)$$

Number of signal (S) and background (B) events, and the corresponding significances with $\alpha_D = 0.1$ are tabulated in Table 3. Evidently, tighter cut on the rapidity y improves the significance considerably. In Table 4, we present the achievable M_D limits for different values of α_D . As discovery criteria, we adopt $S/\sqrt{B} \geq 5$ and $S \geq 25$.

In Fig. 3, the attainable mass limits are presented in the plane (α_D, M_D) . The LHC potential for the discovery of D_2 is clearly demonstrated in Fig. 4 where minimum integrated luminosities, needed to satisfy the adopted criteria, are plotted as a function of M_D for various α_D values.

There are ten different diquarks listed in Table 1, coupled to the first family quarks. All of them will decay into 2 jet final states. Vector and scalar type diquarks can be easily distinguished by the angular distribution of produced jets. To identify different vector (or scalar) diquarks at hadron colliders, one needs polarized proton beams. In principle, electric charge of diquarks can be determined at future lepton and photon colliders, provided that the center of mass energy is larger than $2M_D$. Furthermore, γp colliders based on linac-ring type ep colliders will give essential contribution to the subject. The observation of the associated production of diquarks with leptoquarks will be possible at future lepton-hadron colliders.

In conclusion, the resonance production of vector diquarks at LHC has large cross section. With reasonable cuts, it may be possible to cover mass ranges up to 9 TeV for coupling $\alpha_D = 0.1$. For smaller couplings as $\alpha_D = 5 \times 10^{-4}$, it is still possible to probe diquarks up to the mass of 4 TeV at an integrated luminosity $L = 10^2 \text{fb}^{-1}$.

References

- [1] H. Terazawa, Phys. Rev. 22 (1980) 184; H. Harari, Phys. Rep. 104 (1984) 159; D'Souza and Kalman, Preons, World Scientific Publishing, (1992).
- [2] S. Sultansoy, hep-ph/0003269 (2000).
- [3] J. Wudka, Phys. Lett. B167 (1986) 337.
- [4] J.L. Hewett and T.G. Rizzo, Phys. Rep. 183 (1989) 193.
- [5] F. Abe *et al.*, CDF Collaboration, Phys. Rev. Lett. 77 (1996) 5336; B. Abbott *et al.*, D0 Collaboration, Phys. Rev. Lett. 80 (1998) 666.
- [6] D. Schaile and P.M. Zerwas: Proceedings of the Workshop on Physics at Future Accelerators, CERN Yellow Report 87-07, Vol. II, p.251 (1987).
- [7] T.G. Rizzo, Z. Phys. C43 (1989) 223.
- [8] V.D. Angelopoulos *et al.*, Nucl. Phys. B292, 59 (1987).
- [9] S. Atağ, O. Çakır, and S. Sultansoy, Phys. Rev. D59, 015008 (1998).
- [10] CTEQ Collaboration, H.L. Lai et al., Eur.Phys. J. **C12** (2000) 375.
- [11] Torbjörn Sjöstrand et.al hep-ph/0010017 (2000).
- [12] ATLAS Collaboration, ATLAS TDR 14, CERN/LHCC 99-14 (1999).

Table 1: Quantum numbers of the first generation, color $\bar{3}$ and baryon number $|B| = 2/3$ diquarks described by the effective Lagrangian (5) according to $SU(2)_W \times U(1)_Y$ invariance. $Q_{em} = I_3 + Y/2$

Scalar Diquarks	$SU(2)_W$	$U(1)_Y$	Q_{em}	Couplings
D_1	1	2/3	1/3	$u_L d_L (g_{1L}), u_R d_R (g_{1R})$
\tilde{D}_1	1	-4/3	-2/3	$d_R d_R (\tilde{g}_{1R})$
\tilde{D}'_1	1	8/3	4/3	$u_R u_R (\tilde{g}'_{1R})$
D_3	3	2/3	$\begin{pmatrix} 4/3 \\ 1/3 \\ -2/3 \end{pmatrix}$	$\begin{pmatrix} u_L u_L (\sqrt{2} g_{3L}) \\ u_L d_L (-g_{3L}) \\ d_L d_L (-\sqrt{2} g_{3L}) \end{pmatrix}$
Vector Diquarks				
D_2	2	-1/3	$\begin{pmatrix} 1/3 \\ -2/3 \end{pmatrix}$	$\begin{pmatrix} d_R u_L (g_2) \\ d_R d_L (-g_2) \end{pmatrix}$
\tilde{D}_2	2	5/3	$\begin{pmatrix} 4/3 \\ 1/3 \end{pmatrix}$	$\begin{pmatrix} u_R u_L (\tilde{g}_2) \\ u_R d_L (-\tilde{g}_2) \end{pmatrix}$

Table 2: Cross sections (in pb) for QCD backgrounds contributing to 2 jets final states at parton level, generated by PYTHIA 6.1 with various p_T cuts.

Process	$p_T > 100$ GeV	$p_T > 500$ GeV	$p_T > 1000$ GeV	$p_T > 2000$ GeV
$gg \rightarrow gg$	6.3×10^5	2.0×10^2	2.3×10^0	5.7×10^{-3}
$q_i g \rightarrow q_i g$	6.4×10^5	4.8×10^2	1.0×10^1	5.7×10^{-2}
$q_i q_j \rightarrow q_i q_j$	1.0×10^5	1.8×10^2	6.7×10^0	8.8×10^{-2}
$gg \rightarrow q_k \bar{q}_k$	2.4×10^4	9.8×10^0	1.0×10^{-1}	2.9×10^{-4}
$q_i \bar{q}_i \rightarrow q_k \bar{q}_k$	1.6×10^3	2.8×10^0	1.3×10^{-1}	1.1×10^{-3}
$q_i \bar{q}_i \rightarrow gg$	1.5×10^3	2.5×10^0	6.7×10^{-2}	8.5×10^{-4}
Total	1.4×10^6	8.8×10^2	1.9×10^1	1.5×10^{-1}

Table 3: Observability of the vector diquark D_2 with $\alpha_D = 0.1$ at LHC for $L_{int} = 10^5 \text{pb}^{-1}$.

M_D (TeV)	1	3	5	7	9
$ y_{1,2} < 2$					
S	7.7×10^7	1.1×10^6	5.0×10^4	1.7×10^3	2.7×10^1
B	2.8×10^8	4.2×10^5	8.4×10^3	2.2×10^2	3.1×10^0
S/\sqrt{B}	4585	1768	545	118	16
$ y_{1,2} < 1$					
S	2.6×10^7	5.8×10^5	2.9×10^4	1.1×10^3	1.8×10^1
B	2.5×10^7	4.0×10^4	7.9×10^2	2.1×10^1	3.0×10^{-1}
S/\sqrt{B}	5213	2889	1044	245	34

Table 4: Achievable diquark mass limits for different quark-diquark-quark couplings in the framework of discovery criteria given in the text. $|y_{1,2}| < 2$.

α_D	M_D (TeV)	S	B	S/\sqrt{B}
0.1	9	27	3.1	16.0
0.01	8	25	30	4.6
0.001	5	500	8400	5.4
0.0005	4	1200	54000	5.1

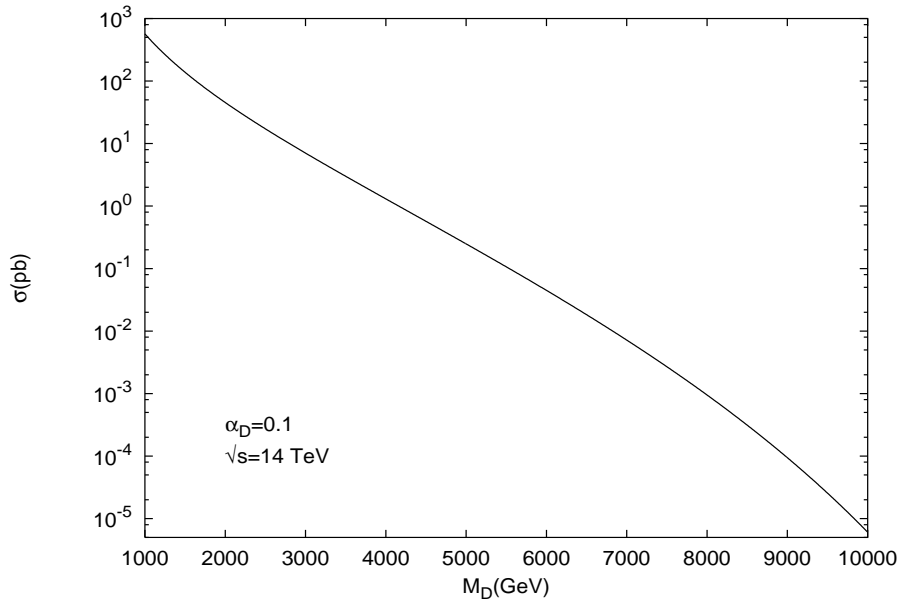


Figure 1: Total cross section versus diquark mass for $\alpha_D = 0.1$.

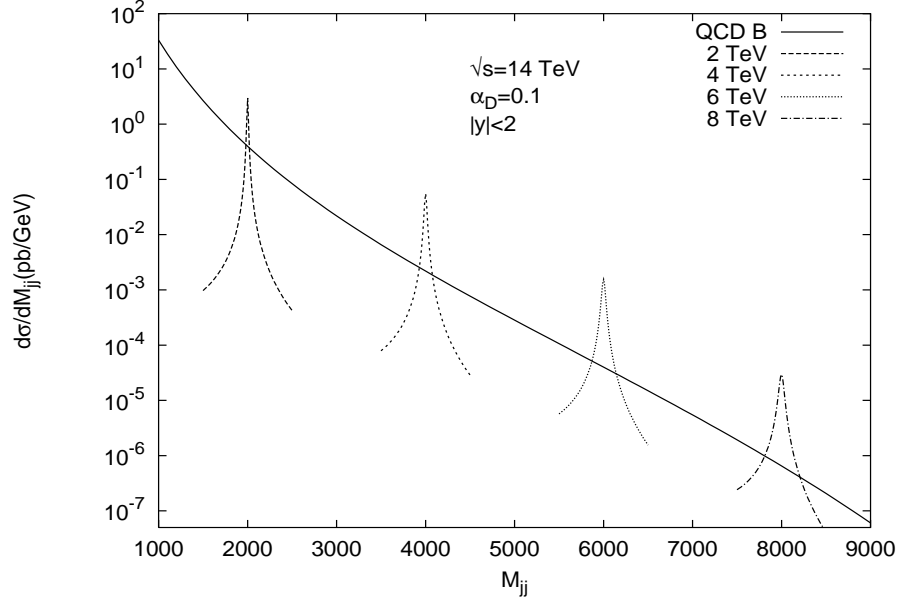


Figure 2: Dijet invariant mass distribution for $M_D = 2, 4, 6, 8$ TeV superimposed over the QCD background.

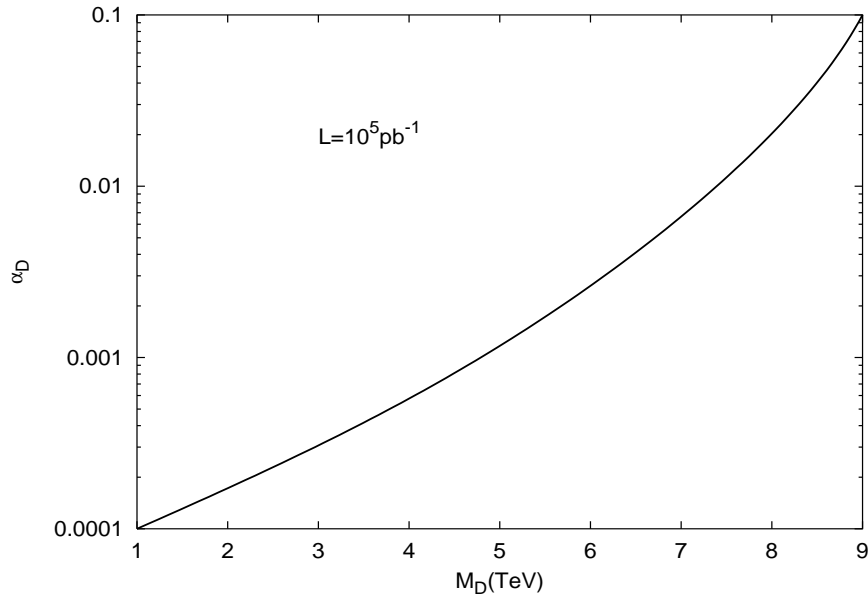


Figure 3: Attainable limits for vector diquark D_2 in α_D - M_D plane.

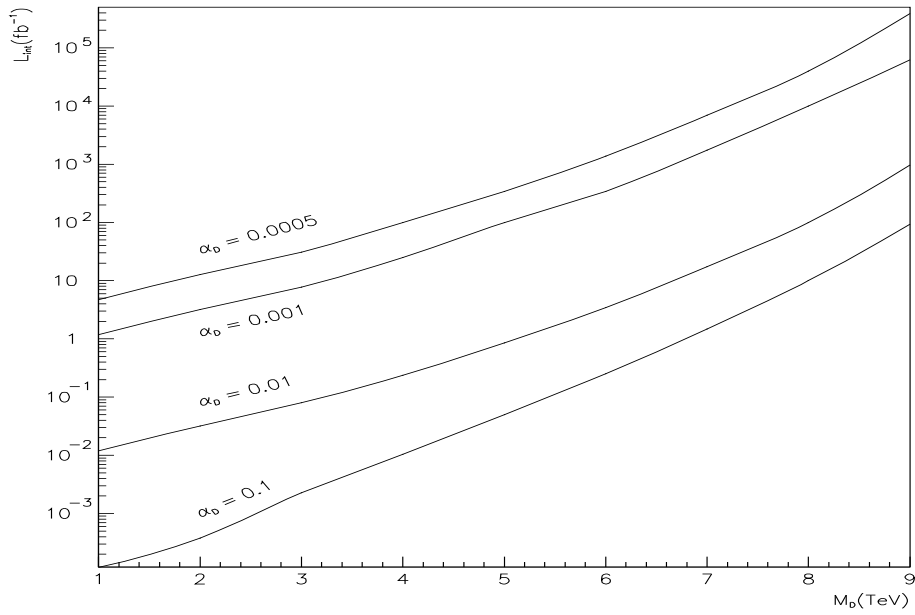


Figure 4: The minimum integrated luminosities, needed to satisfy the adopted discovery criteria, as a function of M_D for various α_D values.